Targeting the p27 E3 ligase SCF^{Skp2} results in p27- and Skp2-mediated cell-cycle arrest and activation of autophagy

Qing Chen,[1] Weilin Xie,[2] Deborah J. Kuhn,[1] Peter M. Voorhees,[1,3] Antonia Lopez-Girona,[2] Derek Mendy,[2] Laura G. Corral,[2] Veronique Plantevin Krenitsky,[2] Weiming Xu,[2] Laure Moutouh-de Parseval,[2] David R. Webb,[2] Frank Mercurio,[2] Keiichi I. Nakayama,[4] Keiko Nakayama,[5] and Robert Z. Orlowski[1,3,6]

[1]Lineberger Comprehensive Cancer Center, University of North Carolina at Chapel Hill; [2]Celgene Signal Research Division, San Diego, CA; [3]Department of Pharmacology, University of North Carolina at Chapel Hill; [4]Department of Molecular and Cellular Biology, Medical Institute of Bioregulation, Kyushu University, Fukuoka, Japan; [5]Division of Developmental Genetics, Tohoku University Graduate School of Medicine, Miyagi, Japan; and [6]Department of Medicine, Division of Hematology/Oncology, University of North Carolina at Chapel Hill

Decreased p27^{Kip1} levels are a poor prognostic factor in many malignancies, and can occur through up-regulation of SCF^{Skp2} E3 ligase function, resulting in enhanced p27 ubiquitination and proteasome-mediated degradation. While proteasome inhibitors stabilize p27^{Kip1}, agents inhibiting SCF^{Skp2} may represent more directly targeted drugs with the promise of enhanced efficacy and reduced toxicity. Using high-throughput screening, we identified Compound A (CpdA), which interfered with SCF^{Skp2} ligase function in vitro, and induced specific accumulation of p21 and other SCF^{Skp2} substrates in cells without activating a heat-shock protein response. CpdA prevented incorporation of Skp2 into the SCF^{Skp2} ligase, and induced G$_1$/S cell-cycle arrest as well as SCF^{Skp2}- and p27-dependent cell killing. This programmed cell death was caspase-independent, and instead occurred through activation of autophagy. In models of multiple myeloma, CpdA overcame resistance to dexamethasone, doxorubicin, and melphalan, as well as to bortezomib, and also acted synergistically with this proteasome inhibitor. Importantly, CpdA was active against patient-derived plasma cells and both myeloid and lymphoblastoid leukemia blasts, and showed preferential activity against neoplastic cells while relatively sparing other marrow components. These findings provide a rational framework for further development of SCF^{Skp2} inhibitors as a novel class of antitumor agents. (Blood. 2008;111: 4690-4699)

© 2008 by The American Society of Hematology

Introduction

The proteasome inhibitor bortezomib (VELCADE, Millennium Pharmaceuticals, Cambridge, MA) has demonstrated significant activity both as a single agent[1,2] and in combination with other drugs[3] against multiple myeloma (MM), validating the ubiquitin-proteasome pathway as a target for cancer therapy. Its broad impact on cellular proteolysis may also have deleterious effects, however, including induction of antiapoptotic heat-shock proteins (HSPs) at the molecular level, and peripheral neuropathy at the clinical level.[4,5] One approach that may overcome these drawbacks would be to target E3 ligases, which are responsible for transfer of ubiquitin moieties to target proteins prior to proteasomal degradation. Since each E3 ligase serves a small subset of protein clients, this would selectively stabilize only those specific proteins, thus minimizing unwanted effects on other targets.[6] SCF complex ligases are the largest family of E3 ligases, and consist of 4 components, including S-phase kinase-associated protein-1 (Skp1), Cullin-1 (Cul1), regulator of cullins-1 (Roc1), and a variable F-box protein.[7] A recent crystal structure of the SCF containing the F-box protein Skp2 (SCF^{Skp2}) revealed that Cul1 served as a scaffold binding a Skp1/Skp2 complex at its N-terminus to recruit substrates, while Roc1 bound at the C-terminus to recruit E2 ubiquitin–conjugating enzymes.[8,9] Since the F-box protein determines the specificity of SCF ligases, it represents a target that could provide the greatest potential selectivity.

Incorporation of Skp2 into an SCF complex confers the ability to induce ubiquitination of several targets, including p27^{Kip1}, p21^{Cip1}, and p57^{Kip2}. As a critical cell-cycle regulator, p27 arrests cell division and inhibits G$_1$/S transition, and cellular p27^{Kip1} levels are largely modulated through the ubiquitin-proteasome pathway. After phosphorylation at Thr187, p27 is recruited to SCF^{Skp2} in the nucleus to be polyubiquitinated for degradation through the 26S proteasome.[10-14] Mutation or silencing of p27 in human cancers is extremely rare,[15] but loss of p27^{Kip1} protein is a common event due to enhanced proteolysis, and has been associated with an aggressive phenotype and a poor prognosis in a variety of malignancies.[16-21] In multiple myeloma, clinical studies have shown that patients with low p27 expression had a significantly shorter overall survival, while patients with high p27^{Kip1} expression receiving high-dose chemotherapy experienced prolonged overall survival.[22-24] Also of note, an accessory protein, Cdc kinase subunit 1 (Cks1), interacts with, and increases binding between, p27^{Kip1} and Skp2.[13] Amplification of the Cks1B locus at 1q21 is associated with a poor prognosis, transformation from monoclonal gammopathy of undetermined significance to MM, and progression of plasma cell leukemia.[23,25] In acute myeloid leukemia (AML) patient specimens, the cytoplasmic to nuclear ratio of p27^{Kip1} is markedly related with the levels of Skp2 expression, and associated with prognosis and disease development.[26] Finally, transient expression

---

of p27^{Kip1} in retinoblastoma protein–defective SaOs-2 cells sensitized them to chemotherapeutic agents,[27] while silencing Skp2 stabilized p27^{Kip1} and suppressed tumor proliferation.[28-30] These data suggest that targeting the SCF^{Skp2} complex to restore p27^{Kip1} levels might be a rational strategy for cancer therapy.

Methods

Cell lines and patient samples

RPMI 8226 and U266 myeloma cells, and their doxorubicin-resistant (RPMI 8226/Dox-40) and melphalan-resistant (RPMI 8226/LR5, U266/LR6) counterparts, were kindly provided by Dr William Dalton (H. Lee Moffitt Cancer Center, Tampa, FL). Dexamethasone-sensitive MM1.S and dexamethasone-resistant MM1.R cells were kindly provided by Dr Steven Rosen (Northwestern University, Evanston, IL). NCI-H929 cells were obtained from the American Type Culture Collection (Manassas, VA), while OPM-2 cells were kindly provided by Dr Gerold Meinhardt (Klinikum der Universität München, Germany). Bortezomib-resistant ANBL-6 cells (ANBL-6/B7R) were generated by serial passage into increasing bortezomib concentrations, and maintained in 7 nM bortezomib. All myeloma cell lines were grown in RPMI 1640 with 100 mM L-glutamine, 10% fetal bovine serum, 1% penicillin/streptomycin, and, where applicable, 1 ng/mL of human recombinant interleukin-6 (IL-6; R&D Systems, Minneapolis, MN). HeLa cells from the University of North Carolina at Chapel Hill (UNC) Tissue Culture Core Facility were maintained in modified Eagle medium (MEM) supplemented as for RPMI 1640. HS-5/GFP bone marrow stromal cells provided by Dr William Dalton were maintained in supplemented RPMI 1640 and with 50 μg/mL hygromycin (Invitrogen, Carlsbad, CA). Wild-type, Skp2$^{-/-}$ knockout, and p27$^{-/-}$ knockout mouse embryo fibroblast (MEF) cells were provided by Dr Keiko Nakayama (Tohoku University, Miyagi, Japan) and Dr Keiichi Nakayama (Kyushu University, Fukuoka, Japan) and maintained in Dulbecco MEM (DMEM) supplemented with 100 mM L-glutamine, 10% fetal bovine serum, 1% sodium pyruvate, and 1% nonessential amino acids.

Primary patient samples were obtained under a University of North Carolina at Chapel Hill Institutional Review Board–approved protocol and with informed consent in accordance with the Declaration of Helsinki. Mononuclear cells from marrow aspirates or peripheral blood were separated using Ficoll-Paque Plus density sedimentation. CD138$^+$ or CD34$^+$ cells were enriched using immunomagnetic beads according to recommended protocols (Miltenyi Biotec, Auburn, CA).

Ubiquitination assay

HeLa cells treated with vehicle or Compound A (CpdA) for 16 hours were lysed in 20 mM HEPES, 5 mM KCl, 1.5 mM MgCl$_2$, and 0.5 mM DTT. Ubiquitination assays were performed using 160 μg cellular extracts with ^{35}S-methionine–labeled in vitro–translated p27 in 40 mM Tris-HCl (pH 7.6), 5 mM MgCl$_2$, 1 mM DTT, 2 μM ubiquitin aldehyde, 1 mg/mL methyl ubiquitin, 10 mM creatine phosphate, 0.1 μg/mL creatine kinase, 0.5 mM ATP, 1 μM okadaic acid, and 2 μg purified active His–cyclin E/Cdk2, with or without 800 ng Skp2/Skp1/Cul1/Roc1 complex as indicated. MM1.S cells were treated with 10 to 25 μM CpdA for 16 hours, and cell lysates were collected. Where indicated, an additional 400 ng His-Cks1 was added to the reactions, which were incubated at 30°C for 2 hours and stopped by adding sample buffer. Products were then separated by denaturing polyacrylamide gel electrophoresis (PAGE) and detected by autoradiography. Unless otherwise indicated, all chemicals were from Sigma-Aldrich (St Louis, MO).

Transient transfection

Complementary oligonucleotides targeting Skp2, 5′-AGCTTTTC-CAAAAAAGGGAGTGACAAAGACTTTGTCTCTTGAACAAAGTC-TTTGTCACTCCCG-3′ and 5′-GATCCGGGAGTGACAAAGACTTTGT-TCAAGAGACAAAGTCTTTGTCACTCCCTTTTTTGGAAA-3′, were synthesized by the UNC Nucleic Acid Core Facility and ligated into

pSilencer 2.1-U6 puro (Ambion, Austin, TX). A negative control in pSilencer expressing a hairpin siRNA, shneg, with limited homology to any known sequences, was provided by Ambion. The hemaglutinin (HA)–tagged-Skp1/pCDNA3.0 plasmid was kindly provided by Dr Joon-Bok Yoon (Yonsei University, Seoul, South Korea). Nucleofector solution R was used for transfection of HeLa cells according to the manufacturer's protocol (Amaxa, Gaithersburg, MD).

Western blotting

Whole-cell extracts were prepared and separated by PAGE as previously described.[31] The antibodies used included anti-Cks1, anti–phospho-(T187)–p27, anti-Skp1, or anti-Skp2 (Zymed Laboratories, South San Francisco, CA); anti-p21 (Abcam, Cambridge, MA); anti–phospho–HSP-27, HSP-27, HSP-70, and HSP-90 (Assay Designs, Ann Arbor, MI); anti–β-catenin, anti–poly-(ADP-ribose) polymerase (PARP), anti–caspase-3, anti–caspase-8, anti–caspase-9, anti-p27, and anti-p57 (Cell Signaling Technology, Danvers, MA); and anti–β-actin, anti–c-Jun, and anti–microtubule-associated protein light chain 3 (MAP-LC3; Santa Cruz Biotechnology, Santa Cruz, CA). For immunoprecipitation, 4 μg anti-HA antibody (Santa Cruz Biotechnology) was added to 500 μg whole-cell extracts, along with 20 μL protein A/G plus beads (Santa Cruz Biotechnology), and incubated overnight. Immunoprecipitates were collected and washed in lysis buffer, boiled in sample buffer, and then subjected to Western blotting.

Growth inhibition assay

Myeloma cells were incubated with CpdA in 2-fold serial dilutions from 2×10^{-5} to 6.25×10^{-7} M. Cells from 3-day cultures were then incubated with the tetrazolium reagent WST-1 (Roche Applied Bioscience, Indianapolis, IN) for 1 to 3 hours, and absorbance was measured at 450 nm, with a reference wavelength of 650 nm. The viability of control cells treated with vehicle was arbitrarily set at 100%.

Caspase inhibition assay

RPMI 8226 cells were preincubated with vehicle or 50 μM PAN-caspase inhibitor (EMD Biosciences, San Diego, CA) for 2 hours before treatment with CpdA or bortezomib, and cell viability was determined after 24 hours as described in "Growth inhibition assay."

Flow cytometric analysis

Myeloma cells cultured in the presence of CpdA or bortezomib were stained with annexin V–fluorescein isothiocyanate (FITC) or annexin V–phycoerythrin (PE; BioVision, Mountain View, CA) as well as the TO-PRO-3 nuclear dye (Invitrogen) for flow cytometry. RPMI 8226 cells treated with both caspase inhibitor or bafilomycin A1 (Sigma-Aldrich), and drugs were double-stained with FITC-VAD-FMK and annexin V–PE and collected for flow cytometry to detect caspase-independent annexin V staining. Propidium iodide (PI) staining was performed to measure cell-cycle progression effects as previously described.[31]

Adhesion of myeloma cells to bone marrow stromal cells

HS-5/GFP stromal cells seeded at 4×10^4 cells/well in 12-well plates were incubated overnight and washed with serum-free medium, and 10^5 MM1.S cells were added, followed by exposure to vehicle, 5 or 10 μM CpdA, or 2.5 nM bortezomib for 18 hours. MM1.S cells were detached by pipetting and stained with annexin V–PE and TO-PRO-3, and a GFP$^-$ population was analyzed by flow cytometry. For dexamethasone treatment, MM1.S cells with or without HS-5/GFP stroma were treated with vehicle or 10 μM dexamethasone in ethanol for 2 days, and analyzed as described in "Flow cytometric analepis."

MDC staining

HeLa cells were treated with dimethyl sulfoxide (DMSO), CpdA alone, or with 200 nM bafilomycin A1 for 4 hours. Monodansylcadaverine (MDC; Sigma-Aldrich) dissolved in 1:1 DMSO/ethanol was added to a final concentration of 100 μM for 1 hour. The cells were then fixed using 4%

A

B

C

D

E

F

G
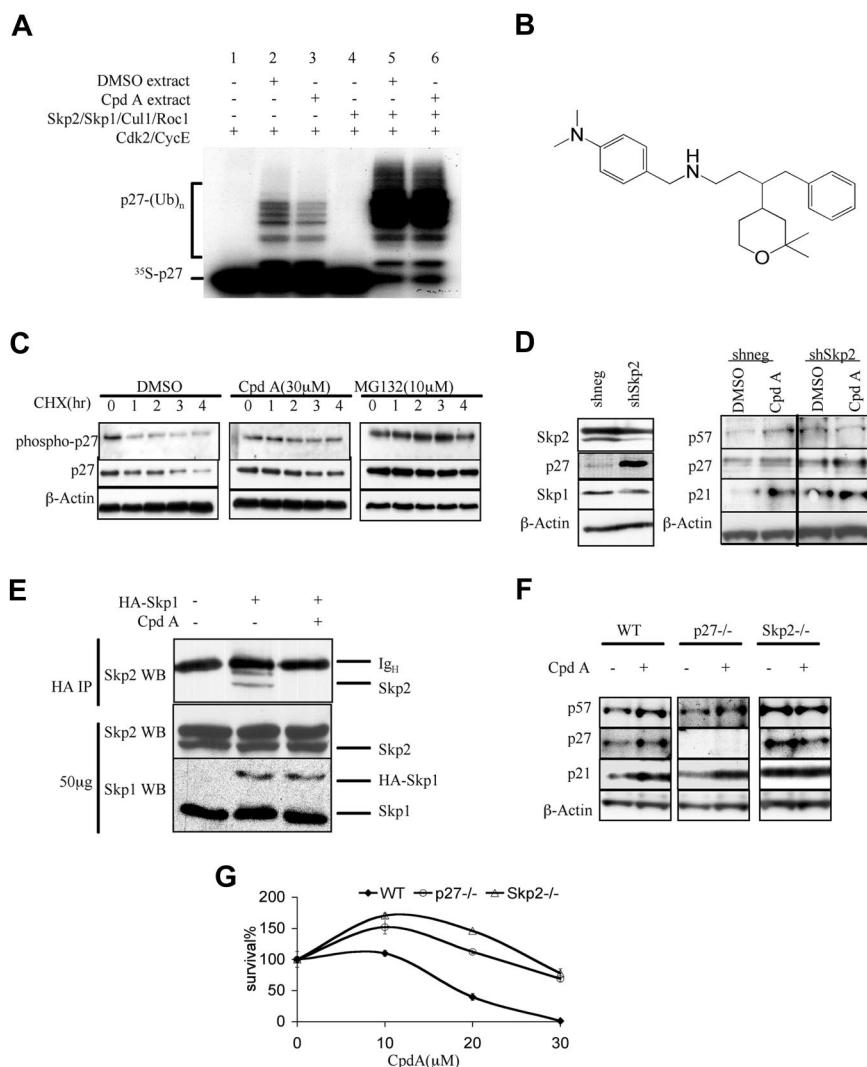
Figure 1. CpdA inhibits p27[Kip1] ubiquitination and turnover. (A) An in vitro–reconstituted system was developed that was capable of modifying labeled p27 (lane 1, 4) into polyubiquinated forms (lane 2). In the presence of 30 μM CpdA, ubiquitination of p27 was inhibited (lane 3). Image J software (http://rsb.info.nih.gov/ij/) measurement showed that CpdA treatment reduced the level of polyubiquitinated p27 to 57% compared with that seen in the vehicle-treated sample (lane 2). Addition of excess Skp2, Skp1, Cul1, and Roc1 restored p27 ubiquination both in the absence of CpdA (lane 5) and in its presence (lane 6), thereby overcoming the activity of Cpd A. (B) The structure of CpdA. (C) HeLa cells arrested in G₁/S phase by double thymidine block were treated with DMSO, 30 μM CpdA, or 10 μM MG132 for 16 hours. Cycloheximide (CHX) was then added for the indicated times, and cell lysates were analyzed by Western blotting to detect p27 and Thr187–phospho-p27. β-actin served as a loading control. (D) HeLa cells were transfected with either a control shRNA (shneg), or an shRNA targeting Skp2 (shSkp2). They were then treated with either vehicle or CpdA for 24 hours, and analyzed by Western blotting for their content of the indicated proteins. (E) HeLa cells were transfected with pcDNA3.0 or pcDNA3.0-HA-Skp1, and then treated with vehicle or 20 μM CpdA for 4 hours. Whole-cell lysates were subjected to immunoprecipitation (IP) with an anti-HA antibody and probed for their Skp2 content. The location of Skp2 and the heavy chain of the precipitating antibody (Ig$_H$) are indicated at the right. As a loading control, 50 μg whole-cell lysates were probed with anti-Skp2 and anti-Skp1 antibodies. (F) WT, p27⁻/⁻, and Skp2⁻/⁻ MEF cells were treated with vehicle or 5 μM CpdA for 24 hours, and analyzed by Western blotting for their content of the indicated proteins. (G) WT, p27⁻/⁻, and Skp2⁻/⁻ MEF cells were treated with vehicle or either 20 μM or 30 μM CpdA for 24 hours; cell viability was assessed using the WST-1 assay. The data shown represent the mean plus or minus standard deviation (SD) of triplicate cultures.

formaldehyde in phosphate-buffered saline (PBS) and visualized by fluorescence microscopy.

Electron microscopy

Cells were harvested after treatment with DMSO, CpdA, or bortezomib, and washed with PBS. Following fixation in 2% paraformaldehyde/2.5% glutaraldehyde, pellets were rinsed and postfixed in 1% osmium tetroxide/1.25% potassium ferrocyanide. Samples were dehydrated in a graded series of ethanols, followed by propylene oxide, and infiltrated and embedded in Polybed 812 resin (Polysciences, Warrington, PA). Thick 1-μm sections were cut with a glass knife, mounted on slides, stained with toluidine blue, and viewed using a light microscope. Ultrathin 70-nm sections were taken from areas selected by light microscopy, mounted on 200 mesh copper grids, and stained with uranyl acetate and lead citrate. These were observed and photographed using a LEO EM-910 transmission electron microscope (LEO Electron Microscopy, Thornwood, NY) at an accelerating voltage of 80 kV.

Statistical analysis

The interaction between anti-MM agents was analyzed using CalcuSyn software (BioSoft, Cambridge, United Kingdom). A combination index (CI) of less than 1.0 indicates synergy, while a CI of 1.0 indicates additive activity. The Student t test was used for other statistical analyses.

Results

Identification of an inhibitor of SCF^{Skp2}-mediated ubiquitination

To screen for compounds that could inhibit p27[Kip1] ubiquitination, we prepared an in vitro–reconstituted system incorporating purified cyclin E/Cdk2, Skp2, Skp1, Cul1, Roc1, and cellular extract from vehicle-treated HeLa cells. This system ubiquitinated ³⁵S-labeled, in vitro–transcribed and –translated p27, as measured by the appearance of a ladder of higher-molecular-weight polyubiquitinated p27[Kip1] (Figure 1A lane 2). After adapting it to a high-throughput format, several libraries were screened, ultimately leading to the identification of CpdA (Figure 1B). In comparison with DMSO-treated cells, reduced in vitro p27 ubiquitination was observed with cell extracts prepared from CpdA-treated HeLa cells (Figure 1A lane 3). Addition of excess, preformed Skp2/Skp1/Cul1/Roc1 overcame inhibition by CpdA, and restored p27 ubiquitination (Figure 1A lane 6), indicating that the SCF^{Skp2} activity in CpdA-treated cells was limited. In order to evaluate the impact of CpdA on p27[Kip1] in a cellular context, HeLa cells were arrested in S phase, exposed to either vehicle, the proteasome inhibitor MG132, or CpdA, then treated with cycloheximide and evaluated for their p27 levels. Compared with vehicle-treated controls (Figure 1C),

MG132 prolonged the half-life of p27 and phospho-p27, as did CpdA (Figure 1C; Figure S1A, available on the *Blood* website; see the Supplemental Materials link at the top of the online article).

To evaluate the mechanism of action of CpdA, HeLa cells were transfected with a control small hairpin interfering RNA (shneg) or one inducing down-regulation of Skp2 (shSkp2; Figure 1D left panel) and then treated with vehicle or CpdA. In HeLa/shneg cells, CpdA induced the accumulation of p27, as well as other SCF^{Skp2} substrates, including p21 and p57 (Figure 1D right panel). However, in HeLa/shSkp2 cells, though as expected basal levels of p21, p27, and p57 were higher compared with HeLa/shneg controls, CpdA did not further increase the levels of these proteins. In order to further test the hypothesis that CpdA was affecting the SCF^{Skp2} complex, HeLa cells were transfected with HA-tagged Skp1 and treated with vehicle or CpdA, and then immunoprecipitation was performed (Figure 1E). Skp2 was detectable in immunoprecipitates from vehicle-treated cells, but was not visible when these had been treated with CpdA, suggesting Skp2 was being excluded from the SCF complex. A dependence on Skp2 was also supported by studies in wild-type (WT), p27$^{-/-}$, and Skp2$^{-/-}$ MEF cells (Figure 1F). CpdA induced p21, p27, and p57 accumulation in WT cells, and p21 and p57 accumulation in p27$^{-/-}$ MEFs, but in Skp2$^{-/-}$ MEFs, CpdA was unable to affect the abundance of these proteins. Also of note, WT MEF cells were treated with increasing CpdA doses, which resulted in a dose-dependent decrease in viability (Figure 1G). Interestingly, Skp2$^{-/-}$ MEFs were more resistant, and even at the highest CpdA doses tested showed only a small decrease compared with vehicle-treated controls. Similarly, p27$^{-/-}$ MEFs were more resistant, though not to the same extent as Skp2$^{-/-}$ cells. Taken together, these studies suggest that this novel agent specifically targets the SCF^{Skp2}-p27 pathway, interferes with the Skp1/Skp2 interaction to prevent SCF^{Skp2} E3 ligase function, and stabilizes p27.

Impact of CpdA in myeloma models

Since the ubiquitin-proteasome pathway has best been validated as a therapeutic target in MM, it was of interest to compare it with CpdA in this context. MM1.S myeloma cells were therefore treated either with vehicle or CpdA, and their extracts were used to catalyze p27 ubiquitination in vitro. As was the case for HeLa cells, CpdA-treated MM1.S cell extracts were less able to catalyze ubiquitination of p27^{Kip1} (Figure 2A left panel) in a dose-dependent fashion. Excess preformed Skp2/Skp1/Cul1/Roc1 complexes overcame inhibition by CpdA (Figure 2A middle panel). Since Cks1 dramatically enhances binding between SCF^{Skp2} and p27, promoting ubiquitination and degradation of p27,[13,23,25,32] we sought to exclude the possibility that Cks1 might also serve as a CpdA target. Excess Cks1 was therefore added, but did not overcome inhibition by CpdA, and did not restore p27 ubiquitination (Figure 2A right panel).

To study the effect of CpdA on intracellular proteolysis, RPMI 8226 cells (Figure 2B) were treated with CpdA or bortezomib. CpdA increased abundance of the SCF^{Skp2} substrates p21^{Cip1}, p27^{Kip1}, and p57^{Kip2} (Figure 2B left panel), as did bortezomib. However, clients of other SCF E3 ligases, such as β-catenin, a target of SCF$^{β-TrCP}$, and c-Jun, a target of SCF^{Fbw7}, were affected only by bortezomib. Notably, the levels of Skp2, Cks1, Cdk2, and Skp1, components of the SCF^{Skp2} complex, were not altered by CpdA (Figure 2B right panel). Finally, bortezomib was seen to activate the HSP response in RPMI 8226 cells (Figure 2C), as evidenced by increased HSP-70 levels, as well as activation of HSP-27 seen as an increase in phospho–HSP-27. Consistent with
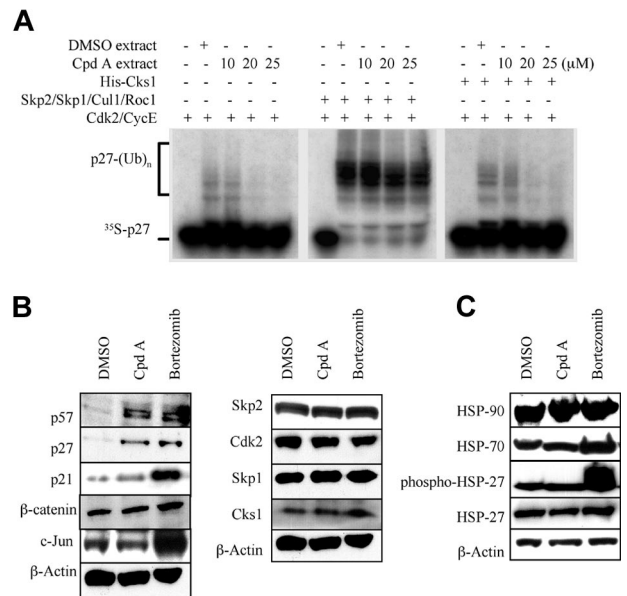

Figure 2. Stabilization of SCF^{Skp2} substrates by CpdA in multiple myeloma cells. (A) Extracts from DMSO- or CpdA-treated MM.1S MM cells were used in the previously detailed p27 in vitro ubiquitination assay to detect inhibition of SCF^{Skp2} E3 ligase function (left panel). Image J software measurement showed that CpdA was again able to inhibit p27 ubiquitination in a dose-dependent fashion in MM1.S cells, with 10-, 20-, and 25-μM concentrations resulting in a reduction of 8%, 44%, and 51% compared with controls. Addition of excess components of SCF^{Skp2} restored ubiquitination (middle panel), but there was no effect on the inhibition of p27 ubiquitination by adding exogenous Cks1 (right panel). (B) RPMI 8226 cells treated with CpdA were then examined for the content of several SCF substrate proteins and cell cycle–related proteins by Western blotting. (C) RPMI 8226 cells were treated with DMSO, CpdA, or bortezomib for 24 hours. Whole-cell lysates were subjected to Western blotting using anti–HSP-27, phospho–HSP-27, HSP-70, and HSP-90 antibodies.

its much more narrow effect on intracellular proteolysis, however, CpdA did not have any of these effects. Similar results were also obtained in MM1.S cells (Figure S1B,C). Taken together, these findings support the hypothesis that this agent, as a novel inhibitor of SCF^{Skp2} E3 ligase function, is much more selective than proteasome inhibitors.

Effect of CpdA on the cell cycle and apoptosis

To study the potential of SCF^{Skp2} as a therapeutic target for MM, a panel of cell lines were treated, and their viability was then evaluated. Inhibition of SCF^{Skp2} resulted in a dose-dependent decrease in viability in all cell lines tested, with 50% inhibition (IC$_{50}$) values in the micromolar range (Figure 3A). Cell-cycle analysis of RPMI 8226 cells was then performed (Figure 3B), and revealed an accumulation of myeloma cells in G$_0$/G$_1$ phase, with a relative paucity of cells traversing through S and G$_2$/M phases. In addition to cell-cycle arrest, CpdA activated programmed cell death (PCD) in a dose-dependent fashion (Figure 3C), as measured by an increase in positive staining with annexin V. Interestingly, while CpdA induced externalization of membrane phosphatidyl-serine residues (Figure 3C), it did not activate type I PCD with oligonucleosomal fragmentation, since flow cytometry revealed no appearance of cells with a sub-G$_1$ DNA content (Figure 3B). Also, bortezomib concentrations that activated PCD to the same extent as did CpdA (Figure 3C) triggered cleavage of caspase-8, caspase-9, and the common effector caspase-3 (Figure 3D), as well as PARP. However, CpdA did not activate either the extrinsic or the intrinsic caspase pathways. Indeed, while survival of myeloma cells after bortezomib was enhanced by preincubation with the PAN-caspase
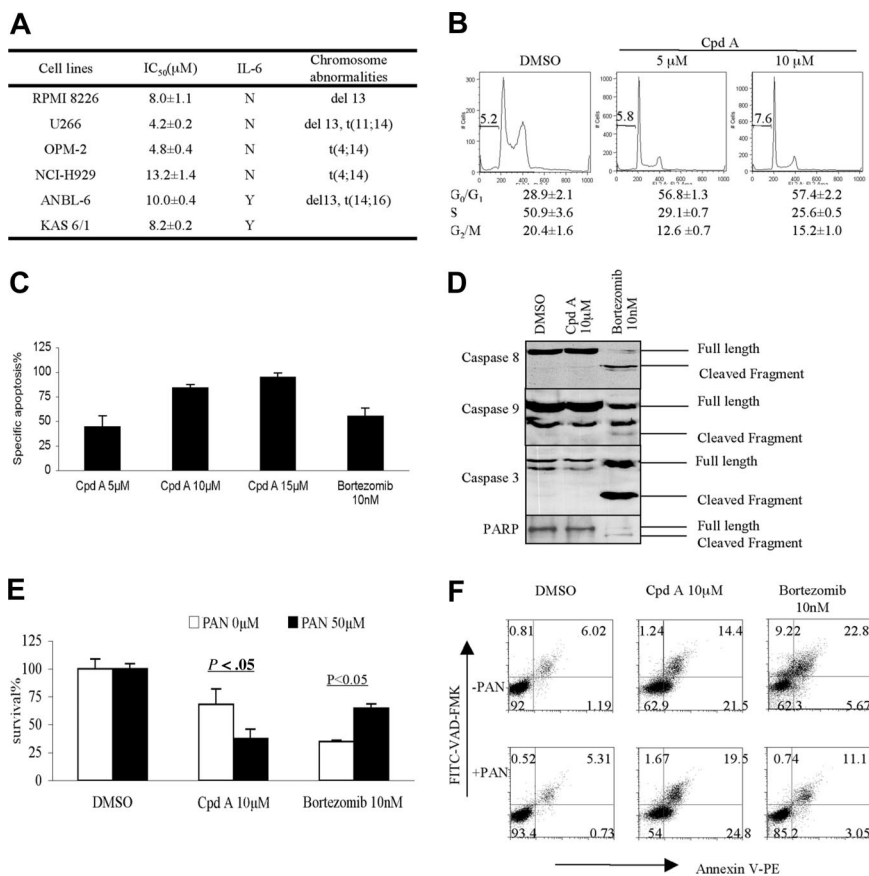
Figure 3. SCF^{Skp2} inhibition induces caspase-independent apoptosis and cell-cycle arrest. (A) A panel of myeloma cell lines was cultured in the presence of varying concentrations of CpdA for 3 days. Cell growth was assessed using the WST-1 assay, and the concentration that induced IC$_{50}$ was calculated. The data shown represent the means plus or minus SD of triplicate cultures. (B) RPMI 8226 cells were treated with vehicle or 5 or 10 µM CpdA for 24 hours. They were then stained with propidium iodide and analyzed by flow cytometry to determine the cell-cycle distribution. (C) RPMI 8226 cells were treated with either 10 nM bortezomib or 5, 10, or 15 µM CpdA, and then analyzed for externalization of phosphatidyl-serine by staining with annexin V. After analysis by flow cytometry, the proportion of specific apoptosis is indicated as the mean plus or minus SD from triplicate experiments. Specific apoptosis was calculated as ((% annexin V$^+$ cells in drug-treated samples − % annexin V$^+$ cells in vehicle-treated controls) / (1 − % annexin V$^+$ cells in vehicle-treated controls)) × 100. (D) Bortezomib- or CpdA-treated RPMI 8226 cells were probed for the presence of full-length and cleaved caspase-8, caspase-9, caspase-3, and PARP by Western blotting. (E) RPMI 8226 cells were preincubated with vehicle or 50 µM PAN-caspase inhibitor for 2 hours, and then treated with vehicle, CpdA, or bortezomib. Cell viability was determined using the WST-1 assay, and is shown as a mean value plus or minus SD from triplicate experiments. (F) Cells treated as described in panel E were analyzed by flow cytometry after staining with annexin V–PE and FITC-VAD-FMK to identify viable cells (PE$^-$/FITC$^-$), as well as those undergoing apoptosis (PE$^+$). The proportion of cells present in the respective quadrants is indicated inside each of the panels. Data are presented from 1 of 3 independent experiments.

inhibitor Z-VAD-FMK (Figure 3E) from 35% to 65% ($P < .05$), PAN-caspase inhibition did not protect cells from CpdA-induced cell death (Figures 3E,S1D). Finally, PAN-caspase inhibition reduced annexin V staining induced by bortezomib nearly to control, vehicle-treated levels (Figure 3F), while no protective effect was seen in regard to CpdA. Thus, CpdA reduced viability and inflicted cell-cycle arrest as well as programmed cell death, but the latter occurred in a caspase-independent manner.

Staining with annexin V can detect caspase-independent apoptosis[33] occurring through type II PCD, or autophagy, and it was therefore of interest to determine if CpdA was activating this pathway. One hallmark of autophagy is the formation of vacuoles that stain with MDC, resulting in a punctate fluorescence. CpdA-treated HeLa cells exhibited this pattern (Figure 4A middle panel), which was suppressed by preincubation with bafilomycin A1, an autophagy inhibitor. Due to the small size of MM cells, analysis for MDC staining at the light microscopic level was unreliable. Using flow cytometry, therefore, we found that CpdA induced the appearance of a large population of annexin V$^+$/caspase-3$^-$ cells (Figure 4B), while bortezomib induced appearance of annexin V$^+$/caspase-3$^+$ cells. Addition of bafilomycin A1 to CpdA significantly increased the viable, annexin V$^-$/caspase-3$^-$ population, while decreasing annexin V$^+$/caspase-3$^-$ cells. Notably, bafilomycin A1 did not inhibit the ability of bortezomib to induce apoptotic annexin V$^+$/caspase-3$^-$ cells, and if anything decreased the proportion of annexin V$^+$/caspase-3$^-$ cells, representing those undergoing autophagy. Another autophagy marker is cleavage of MAP-LC3, a human homolog of the yeast essential autophagy protein Atg8. MAP-LC3-I is processed from its full-length, 18-kDa form to a 16-kDa form, MAP-LC3-II, and the abundance of MAP-LC3-II

reflects the levels of autophagy.[34-36] Incubation of myeloma cells with CpdA enhanced LC3-II formation, indicating autophagic induction (Figures 4C,S1E), while such cleavage was not enhanced in bortezomib-treated cells. Finally, electron microscopy was used to examine the subcellular appearance of myeloma cells undergoing these treatments. Bortezomib induced the appearance of multiple hyperdense intracellular structures (Figure 4D top right panel) consistent with early chromatin condensation and fragmentation, ultimately forming apoptotic bodies. After treatment with CpdA, a different morphology was seen, with numerous double-walled membrane-enclosed cytoplasmic vacuoles. In some sections (Figure 4D bottom right panel), these vacuoles contained intracellular organelles, such as mitochondria. These findings demonstrated that CpdA exerted its antiproliferative and proapoptotic effects through activation of autophagic cell death.

Inhibition of SCF^{Skp2} and drug resistance of CpdA

Targeting SCF^{Skp2} is a possible novel approach to cancer therapy, and given its activity against myeloma it was of interest to determine its potential in overcoming drug resistance and inducing chemosensitization. Melphalan resistance was studied by comparing parental RPMI 8226 and U266 cells, with RPMI 8226/LR5 and U266/LR6 cells, respectively (Figure 5A). Both RPMI 8226 and U266 cells were sensitive to CpdA, and their melphalan-resistant counterparts were sensitive as well, with comparable IC$_{50}$ values. Similar comparisons of RPMI 8226 and RPMI 8226/Dox, and MM1.S and MM1.R cells, showed that CpdA was equally active against the doxorubicin- and steroid-resistant clones, if not more so. The only clinically relevant drug targeting the ubiquitin-proteasome pathway at this time is bortezomib, and we also
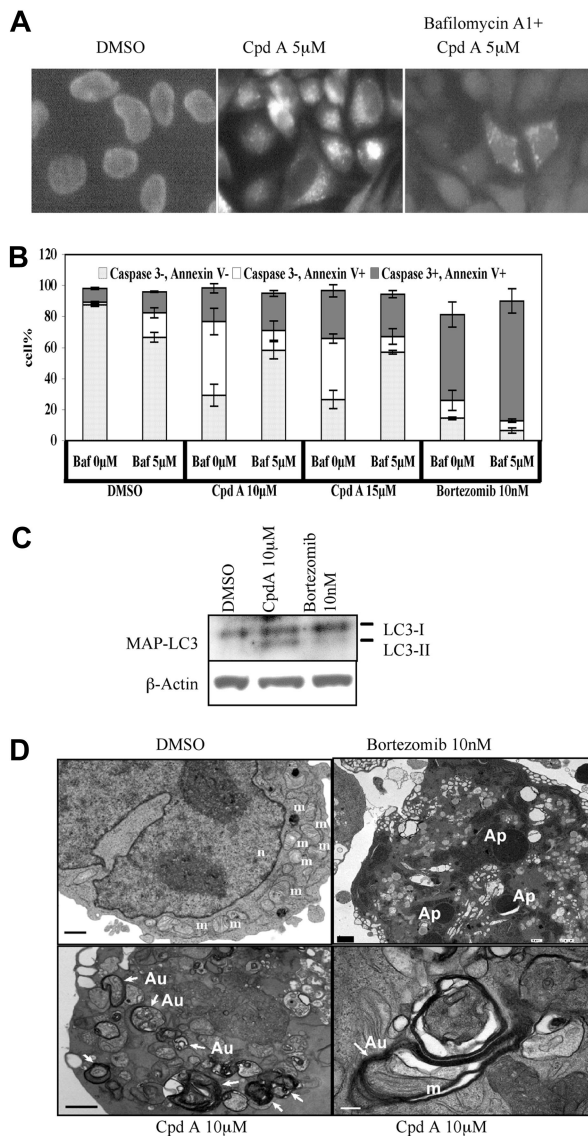
Figure 4. Inhibition of SCF^Skp2 induces autophagic cell death. (A) HeLa cells were treated with vehicle, CpdA at 5μM, or CpdA and 200 nM bafilomycin A1 for 4 hours. They were then stained with MDC and visualized by fluorescence microscopy (Nikon FXA, Nikon, Garden City, NY) using Fluor with iris 40×/1.30 lenses. All images were acquired using QImaging Micropublisher CCD camera (Surrey, BC) and were processed using Adobe Photoshop v8 software (Adobe Systems, San Jose, CA). Note the large amount of punctuate MDC staining after treatment with CpdA (middle panel), which is inhibited by bafilomycin (right panel). (B) RPMI 8226 cells were treated with vehicle, CpdA at 10 or 15 μM, or bortezomib at 10 nM, either alone or with 5 μM bafilomycin, as indicated. They were then evaluated for annexin V staining and caspase 3 activation by flow cytometry. Viable cells are annexin V−/caspase 3−, while those undergoing type I programmed cell death are annexin V+/caspase 3+, and those undergoing autophagy are annexin V+/caspase 3−. Data are represented as the mean percentages of each population plus or minus SD from triplicate experiments. (C) Myeloma cells treated under conditions indicated in Figure 4C for 24 hours were analyzed for their content of LC3-I and LC3-II by Western blotting, with β-actin serving as a loading control. (D) RPMI 8226 cells treated with vehicle, bortezomib, or CpdA were then analyzed by transmission electron microscopy as described in "Electron microscopy". m indicates mitochondria; n, nucleus; and Ap, apoptosomes; white arrows point to autophagic vesicles (Au). The black bar represents 1 μm, and the white bar represents 200 nm.

studied the interactions between that agent and CpdA. Notably, in bortezomib-resistant ANBL-6/B7R cells (Figure 5A), CpdA inhibited proliferation with equal potency to that in WT ANBL-6 cells. Also, when CpdA was added to bortezomib, this combination had enhanced activity against RPMI 8226 (Figure 5B). Isobologram analysis indicated CIs that were consistent with a synergistic

interaction. CpdA was also synergistic with bortezomib against IL-6–dependent KAS-6/1 cells (Figure 5C). Another clinically relevant aspect of MM cells is their expression of adhesion-mediated drug resistance upon interaction with bone marrow stromal cells.[37,38] We next therefore tested whether CpdA could overcome this resistance in MM1.S cells cultured with or without HS-5/GFP stromal cells, and then exposed to CpdA, bortezomib, or dexamethasone. Consistent with previous reports, coculture did protect MM1.S from dexamethasone ($P < .05$), but not from bortezomib-mediated apoptosis (Figure 5D). Similarly, MM1.S cell death induced by CpdA was not suppressed by stromal cells, indicating that agents targeting SCF^Skp2 may overcome multiple drug resistance mechanisms, and induce chemosensitization.
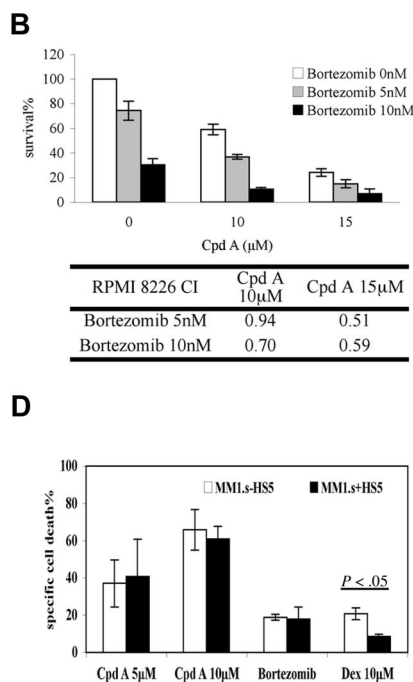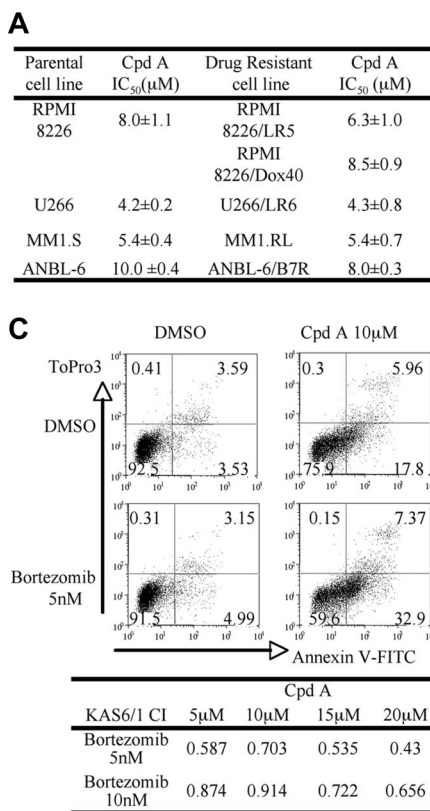
Activity of CpdA against patient-derived malignant cells

To further define the potential efficacy of CpdA, we evaluated its activity against malignant cells freshly isolated from patients with various hematologic malignancies. Plasma cells were purified by CD138+ selection of bone marrow aspirates from patients with MM (Figure 6A). When they were exposed to CpdA, a dose-dependent inhibition of viability was noted in all samples tested. Unsorted bone marrow mononuclear cells were used as a control to evaluate the potential specificity of this agent. A dose-dependent decrease in viability was observed in the CD138+ neoplastic plasma cells (Figure 6B top panels). Importantly, cells that were CD138− (Figure 6B bottom panels), a fraction enriched for nonneoplastic normal bone marrow cells, were less affected. In the CD138+ cell fraction, viability decreased from 66% to 0.3% after treatment, while in CD138− cells, this decreased from 94% to 62%. Similar results were also observed in mononuclear cells from one patient with acute lymphoblastic leukemia (ALL). Viability of CD34+ leukemic blasts decreased from 37.0% to 3.19% after treatment with CpdA (Figure 6C), while in CD34− cells, this decreased from 45.0% to 42.9%.

Elevated Skp2 levels have been described to represent a poor prognostic factor in patients with AML, and it was therefore of interest to examine the activity of CpdA in such samples. Leukemic blasts from the peripheral blood of 2 patients with AML were studied, and on exposure to CpdA both were induced to undergo apoptosis (data not shown). Also, both showed increased abundance of p27^Kip1 (Figure 6D), as did one myeloma patient sample, suggesting that, like bortezomib, CpdA was interfering with p27 turnover. Finally, CpdA was studied in combination with bortezomib, and while both were active in inducing cell death of leukemia blasts alone (Figure 6E), together they acted in a synergistic manner (Figure 6F).

Discussion

Targeting E3 ligases as part of cancer therapy has been proposed as a rational strategy due to the potential for enhanced specificity in comparison with other approaches to modify intracellular proteolysis, such as proteasome inhibition. Overexpression of Skp2 and decreased levels of p27 have been shown to be related to prognosis in a variety of cancers,[39] while silencing of Skp2 to up-regulate p27, or overexpression of p27 itself, inhibited cancer cell proliferation and decreased cell survival.[28-30,40,41] Therefore, the E3 ligase SCF^Skp2 provides a potential drug target for cancer therapy, but pharmacologic inhibitors of its action have not been previously reported.

A

Parental cell line	Cpd A IC$_{50}$(μM)	Drug Resistant cell line	Cpd A IC$_{50}$ (μM)
RPMI 8226	8.0±1.1	RPMI 8226/LR5	6.3±1.0
		RPMI 8226/Dox40	8.5±0.9
U266	4.2±0.2	U266/LR6	4.3±0.8
MM1.S	5.4±0.4	MM1.RL	5.4±0.7
ANBL-6	10.0 ±0.4	ANBL-6/B7R	8.0±0.3

B

RPMI 8226 CI	Cpd A 10μM	Cpd A 15μM
Bortezomib 5nM	0.94	0.51
Bortezomib 10nM	0.70	0.59

C

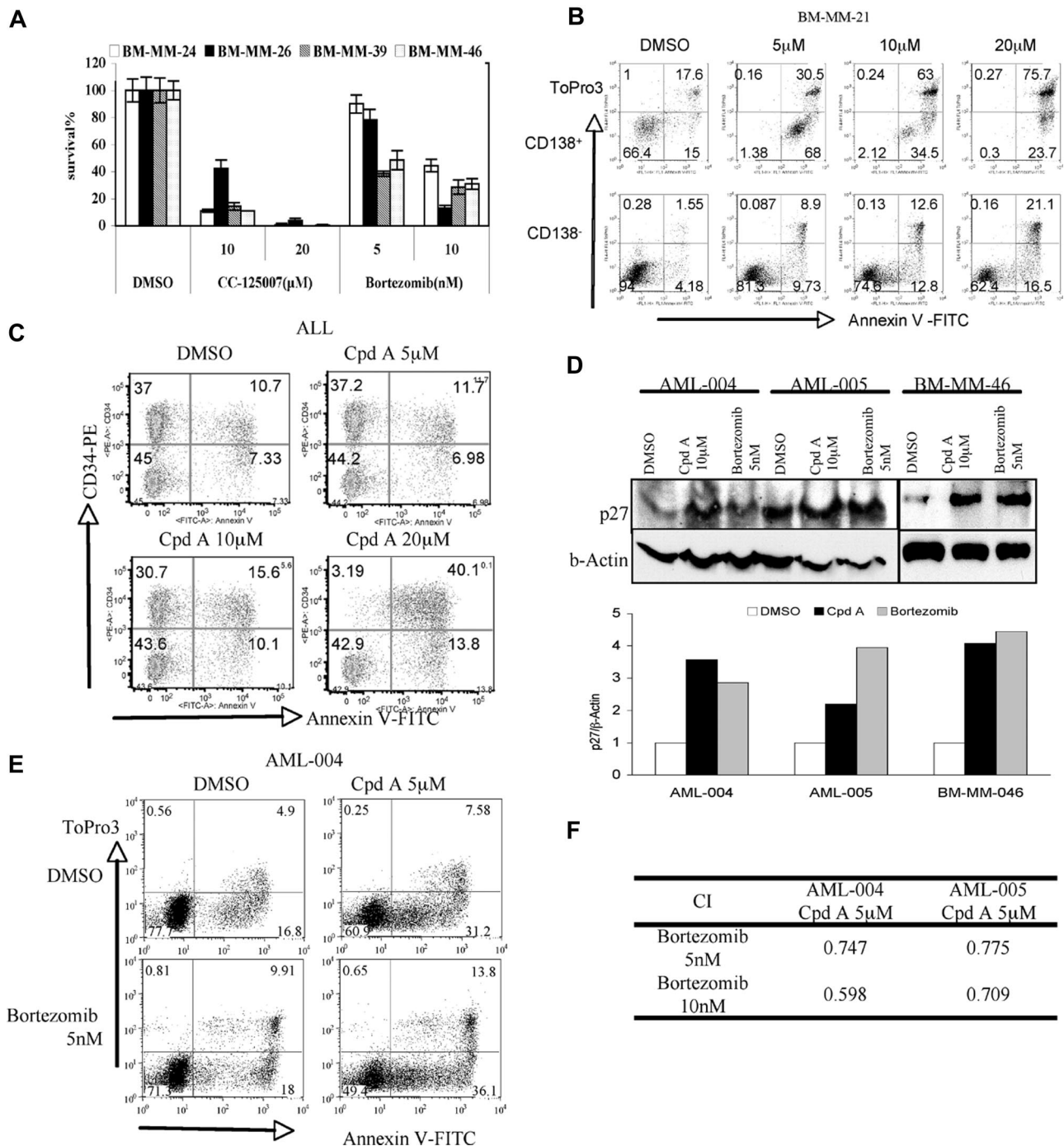|	Cpd A			
KAS6/1 CI	5μM	10μM	15μM	20μM
Bortezomib 5nM	0.587	0.703	0.535	0.43
Bortezomib 10nM	0.874	0.914	0.722	0.656

D

Figure 5. CpdA overcomes drug resistance and induces chemosensitization. (A) Multiple myeloma cell lines RPMI 8226, RPMI 8226/LR5, RPMI 8226/Dox40, U266, U266/LR6, ANBL-6, ANBL-6/B7R, MM1.S, and MM1.R were cultured with CpdA for 3 days, and cell viability was determined as described previously. Data represent the mean IC$_{50}$ plus or minus SD of triplicate cultures. (B) RPMI 8226 cells were treated with the indicated concentrations of bortezomib alone or together with 10 or 15 μM of CpdA for 24 hours, and then analyzed for viability using the WST-1 assay (top panel). CI values are shown in the table (bottom panel), with values of 0.9 or less indicating synergy. (C) IL-6–dependent KAS-6/1 myeloma cells were treated with bortezomib or CpdA alone or together for 24 hours, and then analyzed for staining with annexin V–FITC and TO-PRO-3 by flow cytometry. The proportion of cells present in the respective quadrants is indicated inside each of the panels, including viable cells (FITC⁻/To Pro3⁻), early apoptotic cells (FITC⁺/To Pro3⁻), and late apoptotic or necrotic cells (FITC⁺/To Pro3⁺). (D) MM.1S myeloma cells were plated either in the absence or presence of HS-5/GFP stromal cells, and then exposed to the indicated concentrations of CpdA or bortezomib for 18 hours or dexamethasone for 48 hours. The proportion of viable cells was then evaluated by flow cytometry. Specific cell death is represented as the mean plus or minus SD of triplicate experiments.

In the current work, we report the identification of a small molecule that inhibited in vitro p27 ubiquitination, and also stabilized p27 in cell-line model systems (Figures 1,2,S1). Other SCF^{Skp2} complex substrates, such as p21 and p57, were also stabilized, while substrates of different SCF E3 ligases were unaffected (Figures 2,S1). The narrower effect of this agent on intracellular proteolysis was demonstrated by a lack of accumulation of ubiquitin-protein conjugates (data not shown), and a lack of activation of the HSP response (Figures 2,S1). When gene expression profiles of DMSO- and CpdA-treated RPMI 8226 cells were compared, there were only 78 genes that showed an at least 2-fold change (data not shown), and since p27 was not among them, accumulation of p27 was not due to up-regulation of messenger expression. This further indicates that, unlike the proteasome inhibitor bortezomib, which had a much broader impact on gene expression profiles,[4,42] CpdA had a comparatively limited effect on transcriptional activity. Mechanistic studies suggested that inhibition of p27 ubiquitination by CpdA involved direct targeting of SCF^{Skp2} E3 ligase function by excluding Skp2 from the SCF complex, in that immunoprecipitation failed to identify this F-box protein when Skp1 was isolated in the presence of this compound, compared with controls (Figure 1E). Since Skp2 expression itself was not affected, CpdA may act by disrupting binding between Skp1 and Skp2. MEF cell studies further indicated that CpdA-induced cell death was mainly due to its effect on the SCF^{Skp2}-p27 pathway, since p27$^{-/-}$ MEFs showed only a slightly smaller degree of resistance to CpdA than Skp2$^{-/-}$ MEFs. Recent studies have shown that neddylation of Cul1 is an important step in assembly of this E3 ligase,[43] and that cyclin D1 and the phosphatase and tensin homolog on chromosome 10 may also play roles.[44] It is therefore possible that CpdA may function through other mechanisms, such as by interfering with Cul1 neddylation.

Further studies will be needed, and are ongoing, to better define the pathways affected by CpdA and its homologs.

Inhibition of SCF^{Skp2} blocked proliferation of neoplastic cells by inducing G$_1$/S cell-cycle arrest and apoptosis (Figure 3). Interestingly, the latter did not occur through caspase-mediated pathways, since proteolytic cleavage of caspase-8, caspase-9, and caspase-3 was not seen, and PAN-caspase inhibition did not suppress apoptosis. Instead, CpdA activated type II PCD, or autophagy, based on the appearance of MDC cell staining and annexin V$^+$/caspase-3$^-$ cell populations, both of which were suppressed by bafilomycin A1 (Figure 4). Moreover, proteolytic processing of MAP-LC3 and electron microscopy showing the appearance of autophagic vacuoles also supported this conclusion. Up-regulation of p27 via mammalian target of rapamycin inhibition has been described to induce cell-cycle arrest at the G$_0$/G$_1$ phase in association with the induction of autophagy.[45] Also, direct overexpression of p27 in cancer cells induced autophagy[40,41] and showed a greater antitumor effect than did the overexpression of other cyclin-dependent kinase inhibitors.[40] This suggests that stabilization of p27 by CpdA may be responsible for activation of type II PCD, but additional studies will be needed in this regard. The transcriptional profile of CpdA-treated cells showed up-regulation of the autophagy gene human WD-repeat protein interacting with phosphoinosides (h-WIPI-1α), a human homolog of the yeast Atg18 gene,[46] which is vital for all forms of autophagy in *Saccharomyces cerevisiae*.[47] Studies have shown that hWIPI-1 could colocalize in part with the autophagosomal marker LC3 at punctate cytoplasmic structures, and the accumulation of hWIPI-1 in cytoplasmic vesicular structures occurred during amino acid deprivation–induced autophagy.[46] Thus, direct or indirect induction of WIPI49 by CpdA may also contribute to activation of type II PCD.

Figure 6. CpdA is active in patient-derived neoplastic cells. (A) Plasma cells (CD138$^+$) were purified from 3 unique patient bone marrow aspirates and incubated with CpdA or bortezomib for 2 days under the indicated conditions. Viability was determined using the WST-1 assay, and is represented as the mean plus or minus SD from triplicate experiments. (B) The mononuclear cell fraction from a fourth patient with myeloma was cultured with DMSO or the indicated concentration of CpdA for 24 hours; stained with CD138-PE, annexin V–FITC, and TO-PRO-3; and analyzed by flow cytometry. CD138$^+$ myeloma cells are gated in the top row, while CD138$^-$ cells are gated in the bottom row. The proportion of cells present in the respective quadrants is indicated inside each of the panels, including viable cells (FITC$^-$/To Pro3$^-$), early apoptotic cells (FITC$^+$/To Pro3$^-$), and late apoptotic or necrotic cells (FITC$^+$/To Pro3$^+$). (C) Mononuclear cells isolated from the peripheral blood of a patient with CD34$^+$ acute lymphoblastic leukemia were cultured with DMSO and CpdA for 24 hours, then stained with CD34-PE and annexin V–FITC and analyzed by flow cytometry. The proportion of cells present in the respective quadrants is indicated inside each panel as described for panel B. (D) Mononuclear cells isolated from 2 unique patients with AML and one patient with MM were cultured with DMSO, 10 μM CpdA, or 5 nM bortezomib for 24 hours. Whole-cell lysates were subject to Western blotting (top panel) using anti-p27 and β-actin antibodies, and analyzed by densitometry (bottom panel). (E) Isolates from a patient with AML were cultured with the indicated concentration of bortezomib, CpdA, or the combination for 24 hours. Cells were then stained with annexin V–FITC and TO-PRO-3 and analyzed using flow cytometry. The proportion of cells present in the respective quadrants is indicated inside each panel as for panel B. (F) Isobologram analysis of the viability results when leukemia patient samples were treated with combinations of bortezomib and CpdA.

Autophagy is necessary for survival of cells under unfavorable conditions to recycle microorganelles, but it may also induce cell death when excessive autophagy occurs. A number of studies have

reported that this pathway is activated in cancer cells in response to DNA-damaging agents and other anticancer therapies,[48-50] such as arsenic trioxide, rapamycin, and tamoxifen. Combinations of

autophagy-inducing agents and proteasome inhibitors have shown synergistic cell killing.[51] This provided a rationale for combining CpdA with bortezomib, and indeed, CpdA and bortezomib were found to be synergistic (Figure 5), and CpdA even overcame resistance to bortezomib. The basis for this synergy may be the ability of CpdA to prevent turnover of the polyubiquitinated proteins accumulated by proteasome inhibition through the autophagic pathway, thus targeting major nonlysosomal and lysosomal protein degradation mechanisms. Alternatively, synergy may be a result of this combination's ability to activate both caspase-dependent and -independent apoptosis.

Understanding the mechanism of action of agents such as CpdA may allow us to rationally design new methods of treatment using this compound in combination with other anticancer drugs. Interestingly, CpdA did not enhance the effects of either melphalan or doxorubicin (data not shown). As a DNA cross-linker, melphalan targets S-phase DNA and delays cell-cycle progression into the G_2/M phase,[31] while CpdA arrests the cell cycle at G_0/G_1. One possible explanation for this is that SCF^{Skp2} inhibition prevented cells from entering S phase, and therefore protected them from DNA damage by melphalan. It is not yet clear why the combination of CpdA and doxorubicin were not synergistic in MM cells. It has been observed that overexpression of p27 in human colon cancer cells decreased their tumorigencity in nude mice, however, and the p27-overexpressing tumors were more resistant to intraveneous doxorubicin.[52] Furthermore, in MCF-7 breast cancer cells, subcellular distribution of p27 was associated with cross-resistance to doxorubicin.[53] These studies indicate that accumulation of p27 might have negative consequences in treatment outcomes with anthracyclines. Another recent study showed that p27 was stabilized in non-Hodgkin lymphomas when cells were adhered to bone marrow stromal cells. The accumulation of p27 was due to down-regulation of the SCF^{Skp2} E3 ligase pathway.[38] Our study showed that although CpdA targeted the SCF^{Skp2}-p27 pathway, the agent was able to overcome stroma-mediated drug resistance.

Finally, we were able to document activity of CpdA in neoplastic cell populations from patients with MM, ALL, and AML, with evidence of relative sparing of nonneoplastic cells (Figure 6). Of the 4 patients with myeloma examined, MM-24, MM-26, and MM-39 had 13q deletions and were bortezomib-naive, while MM-21 had clinically progressed on a bortezomib-based regimen. These studies suggest that CpdA has the potential for activity in clinically high-risk patients with myeloma, and may overcome clinical bortezomib resistance. Similarly, patient AML-004 had relapsed disease after prior induction therapy with daunorubicin, cytarabine, and etoposide, followed by consolidation with high-dose cytarabine. Given the role of p27 as a prognostic factor in patients with solid tumors as well, we have evaluated the activity of CpdA in other cell lines, and found activity against models of breast cancer, prostate cancer, and glioma, among others, again with evidence of induction of autophagy (data not shown). One limitation of this agent is its relative lack of potency, in that it requires micromolar concentrations for efficacy, limiting the ability to perform in vivo studies. We are currently evaluating stereoisomers of this compound that seem to have enhanced potency, and structure activity relationship studies may help in optimizing its structure further. These studies do provide a proof of principle, however, provide a framework for further development of agents such as CpdA that target SCF^{Skp2}, and support their great potential to become important parts of our future chemotherapeutic armamentarium against a variety of malignancies.

Acknowledgments

Authorship

Contribution: Q.C. designed and performed the majority of the research and wrote the manuscript; W.X., A.L.-G., D.M., L.G.C., V.P.K., W.X., L.M.-d.P., D.R.W., and F.M. were involved in the compound screening, chemical synthesis, and ubiquitination assays; D.J.K. and P.M.V. were essential for helping with patient sample purifications; K.I.N. and K.N. provided MEF WT, p27$^{-/-}$, and Skp2$^{-/-}$ knockout cells; and R.Z.O. supervised all the research and wrote the manuscript.

Conflict-of-interest disclosure: W.X., A.L.-G., D.M., L.G.C., V.P.K., W.X., L.M.-d.P., D.R.W., and F.M. are employees of Celgene, and receive stock options as part of their employment. All other authors declare no competing financial interests.

Correspondence: Robert Z. Orlowski, The University of Texas M. D. Anderson Cancer Center, Department of Lymphoma/Myeloma, 1515 Holcombe Blvd, Unit 429, Houston, TX 77030-4009; e-mail: rorlowsk@mdanderson.org.

References

1. Richardson PG, Barlogie B, Berenson J, et al. A phase 2 study of bortezomib in relapsed, refractory myeloma. N Engl J Med. 2003;348:2609-2617.

2. Richardson PG, Sonneveld P, Schuster MW, et al. Bortezomib or high-dose dexamethasone for relapsed multiple myeloma. N Engl J Med. 2005; 352:2487-2498.

3. Orlowski RZ, Nagler A, Sonneveld P, et al. Randomized phase III study of pegylated liposomal doxorubicin plus bortezomib compared with bortezomib alone in relapsed or refractory multiple myeloma: combination therapy improves time to progression. J Clin Oncol. 2007;25: 3892-3901.

4. Mitsiades N, Mitsiades CS, Poulaki V, et al. Molecular sequelae of proteasome inhibition in human multiple myeloma cells. Proc Natl Acad Sci U S A. 2002;99:14374-14379.

5. Richardson PG, Briemberg H, Jagannath S, et al. Frequency, characteristics, and reversibility of peripheral neuropathy during treatment of advanced multiple myeloma with bortezomib. J Clin Oncol. 2006;24:3113-3120.

6. Sun Y. Targeting E3 ubiquitin ligases for cancer therapy. Cancer Biol Ther. 2003;2:623-629.

7. Nakayama KI, Nakayama K. Regulation of the cell cycle by SCF-type ubiquitin ligases. Semin Cell Dev Biol. 2005;16:323-333.

8. Zheng N, Schulman BA, Song L, et al. Structure of the Cul1-Rbx1-Skp1-F boxSkp2 SCF ubiquitin ligase complex. Nature. 2002;416:703-709.

9. Hao B, Zheng N, Schulman BA, et al. Structural basis of the Cks1-dependent recognition of p27(Kip1) by the SCF(Skp2) ubiquitin ligase. Mol Cell. 2005;20:9-19.

10. Carrano AC, Eytan E, Hershko A, Pagano M. SKP2 is required for ubiquitin-mediated degradation of the CDK inhibitor p27. Nat Cell Biol. 1999; 1:193-199.

11. Sutterluty H, Chatelain E, Marti A, et al. p45SKP2 promotes p27Kip1 degradation and induces S phase in quiescent cells. Nat Cell Biol. 1999;1: 207-214.

12. Harper JW. Protein destruction: adapting roles for Cks proteins. Curr Biol. 2001;11:R431-R435.

13. Ganoth D, Bornstein G, Ko TK, et al. The cell-cycle regulatory protein Cks1 is required for SCF-(Skp2)-mediated ubiquitinylation of p27. Nat Cell Biol. 2001;3:321-324.

14. Spruck C, Strohmaier H, Watson M, et al. A CDK-independent function of mammalian Cks1: targeting of SCF(Skp2) to the CDK inhibitor p27Kip1. Mol Cell. 2001;7:639-650.

15. Slingerland J, Pagano M. Regulation of the cdk inhibitor p27 and its deregulation in cancer. J Cell Physiol. 2000;183:10-17.

16. Catzavelos C, Bhattacharya N, Ung YC, et al. Decreased levels of the cell-cycle inhibitor p27Kip1 protein: prognostic implications in primary breast cancer. Nat Med. 1997;3:227-230.

17. Masciullo V, Ferrandina G, Pucci B, et al. p27Kip1 expression is associated with clinical outcome in advanced epithelial ovarian cancer: multivariate analysis. Clin Cancer Res. 2000;6:4816-4822.

18. Yang RM, Naitoh J, Murphy M, et al. Low p27 expression predicts poor disease-free survival in patients with prostate cancer. J Urol. 1998;159: 941-945.

19. Esposito V, Baldi A, De Luca A, et al. Prognostic role of the cyclin-dependent kinase inhibitor p27 in non-small cell lung cancer. Cancer Res. 1997; 57:3381-3385.

20. Han S, Kim HY, Park K, Lee MS, Kim HJ, Kim YD. Expression of p27Kip1 and cyclin D1 proteins is inversely correlated and is associated with poor clinical outcome in human gastric cancer. J Surg Oncol. 1999;71:147-154.

21. Tae Kim Y, Kyoung Choi E, Hoon Cho N, et al. Expression of cyclin E and p27(KIP1) in cervical carcinoma. Cancer Lett. 2000;153:41-50.

22. Filipits M, Pohl G, Stranzl T, et al. Low p27Kip1 expression is an independent adverse prognostic factor in patients with multiple myeloma. Clin Cancer Res. 2003;9:820-826.

23. Shaughnessy J. Amplification and overexpression of CKS1B at chromosome band 1q21 is associated with reduced levels of p27Kip1 and an aggressive clinical course in multiple myeloma. Hematology. 2005;10:117-126.

24. Filipits M, Puhalla H, Wrba F. Low p27Kip1 expression is an independent prognostic factor in gallbladder carcinoma. Anticancer Res. 2003;23: 675-679.

25. Chang H, Yeung J, Xu W, Ning Y, Patterson B. Significant increase of CKS1B amplification from monoclonal gammopathy of undetermined significance to multiple myeloma and plasma cell leukaemia as demonstrated by interphase fluorescence in situ hybridisation. Br J Haematol. 2006; 134:613-615.

26. Min YH, Cheong JW, Lee MH, et al. Elevated S-phase kinase-associated protein 2 protein expression in acute myelogenous leukemia: its association with constitutive phosphorylation of phosphatase and tensin homologue protein and poor prognosis. Clin Cancer Res. 2004;10:5123-5130.

27. Gabellini C, Pucci B, Valdivieso P, et al. p27(kip1) overexpression promotes paclitaxel-induced apoptosis in pRb-defective SaOs-2 cells. J Cell Biochem. 2006;98:1645-1652.

28. Kudo Y, Kitajima S, Ogawa I, Kitagawa M, Miyauchi M, Takata T. Small interfering RNA targeting of S phase kinase-interacting protein 2 inhibits cell growth of oral cancer cells by inhibiting p27 degradation. Mol Cancer Ther. 2005;4:471-476.

29. Jiang F, Caraway NP, Li R, Katz RL. RNA silencing of S-phase kinase-interacting protein 2 inhibits proliferation and centrosome amplification in lung cancer cells. Oncogene. 2005;24:3409-3418.

30. Katagiri Y, Hozumi Y, Kondo S. Knockdown of Skp2 by siRNA inhibits melanoma cell growth in vitro and in vivo. J Dermatol Sci. 2006;42:215-224.

31. Chen Q, Van der Sluis PC, Boulware D, Hazlehurst LA, Dalton WS. The FA/BRCA pathway is involved in melphalan-induced DNA interstrand cross-link repair and accounts for melphalan resistance in multiple myeloma cells. Blood. 2005; 106:698-705.

32. Zhan F, Colla S, Wu X, et al. CKS1B, overexpressed in aggressive disease, regulates multiple myeloma growth and survival through SKP2- and p27Kip1-dependent and -independent mechanisms. Blood. 2007;109:4995-5001.

33. Cummings BS, Kinsey GR, Bolchoz LJ, Schnellmann RG. Identification of caspase-independent apoptosis in epithelial and cancer cells. J Pharmacol Exp Ther. 2004;310:126-134.

34. Mizushima N. Methods for monitoring autophagy. Int J Biochem Cell Biol. 2004;36:2491-2502.

35. Wu H, Yang JM, Jin S, Zhang H, Hait WN. Elongation factor-2 kinase regulates autophagy in human glioblastoma cells. Cancer Res. 2006;66: 3015-3023.

36. Asanuma K, Tanida I, Shirato I, et al. MAP-LC3, a promising autophagosomal marker, is processed during the differentiation and recovery of podocytes from PAN nephrosis. FASEB J. 2003;17: 1165-1167.

37. Schmidmaier R, Baumann P, Simsek M, Dayyani F, Emmerich B, Meinhardt G. The HMG-CoA reductase inhibitor simvastatin overcomes cell adhesion-mediated drug resistance in multiple myeloma by geranylgeranylation of Rho protein and activation of Rho kinase. Blood. 2004;104:1825-1832.

38. Lwin T, Hazlehurst LA, Dessureault S, et al. Cell adhesion induces p27Kip1-associated cell-cycle arrest through down-regulation of the SCFSkp2 ubiquitin ligase pathway in mantle cell and other non-Hodgkin B-cell lymphomas. Blood. 2007;110: 1631-1638.

39. Nakayama KI, Nakayama K. Ubiquitin ligases: cell-cycle control and cancer. Nat Rev Cancer. 2006;6:369-381.

40. Komata T, Kanzawa T, Takeuchi H, et al. Antitumour effect of cyclin-dependent kinase inhibitors (p16(INK4A), p18(INK4C), p19(INK4D), p21(WAF1/CIP1) and p27(KIP1)) on malignant glioma cells. Br J Cancer. 2003;88:1277-1280.

41. Liang J, Shao SH, Xu ZX, et al. The energy sensing LKB1-AMPK pathway regulates p27(kip1) phosphorylation mediating the decision to enter autophagy or apoptosis. Nat Cell Biol. 2007;9: 218-224.

42. Mitsiades N, Mitsiades CS, Richardson PG, et al. The proteasome inhibitor PS-341 potentiates sensitivity of multiple myeloma cells to conventional chemotherapeutic agents: therapeutic applications. Blood. 2003;101:2377-2380.

43. Bornstein G, Ganoth D, Hershko A. Regulation of neddylation and deneddylation of cullin1 in SCF-Skp2 ubiquitin ligase by F-box protein and substrate. Proc Natl Acad Sci U S A. 2006;103: 11515-11520.

44. Jonason JH, Gavrilova N, Wu M, Zhang H, Sun H. Regulation of SCF(SKP2) ubiquitin E3 ligase assembly and p27(KIP1) proteolysis by the PTEN pathway and Cyclin D1. Cell Cycle. 2007;6:951-961.

45. Georgakis GV, Yazbeck VY, Li Y, Younes A. The mTOR inhibitor temsirolimus (CCI-779) induces cell cycle arrest and autophagy in Hodgkin lymphoma (HL) cell lines and enhances the effect of the PI3-kinase inhibitor LY294002 [abstract]. Blood. 2006;108:639a. Abstract no. 2259.

46. Proikas-Cezanne T, Waddell S, Gaugel A, Frickey T, Lupas A, Nordheim A. WIPI-1alpha (WIPI49), a member of the novel 7-bladed WIPI protein family, is aberrantly expressed in human cancer and is linked to starvation-induced autophagy. Oncogene. 2004;23:9314-9325.

47. Stromhaug PE, Reggiori F, Guan J, Wang CW, Klionsky DJ. Atg21 is a phosphoinositide binding protein required for efficient lipidation and localization of Atg8 during uptake of aminopeptidase I by selective autophagy. Mol Biol Cell. 2004;15: 3553-3566.

48. Kondo Y, Kanzawa T, Sawaya R, Kondo S. The role of autophagy in cancer development and response to therapy. Nat Rev Cancer. 2005;5:726-734.

49. Kanzawa T, Zhang L, Xiao L, Germano IM, Kondo Y, Kondo S. Arsenic trioxide induces autophagic cell death in malignant glioma cells by upregulation of mitochondrial cell death protein BNIP3. Oncogene. 2005;24:980-991.

50. Kanzawa T, Germano IM, Komata T, Ito H, Kondo Y, Kondo S. Role of autophagy in temozolomide-induced cytotoxicity for malignant glioma cells. Cell Death Differ. 2004;11:448-457.

51. Zhou Y, Yau C, Gray JW, et al. Enhanced NF kappa B and AP-1 transcriptional activity associated with antiestrogen resistant breast cancer. BMC Cancer. 2007;7:59.

52. Dimanche-Boitrel MT, Micheau O, France D, et al. P27KiP1 overexpression inhibits the growth and doxorubicin sensitivity of HT29 human colon cancer cells in vivo. Anticancer Res. 2000;20: 849-852.

53. Wang Z, Kishimoto H, Bhat-Nakshatri P, Crean C, Nakshatri H. TNFalpha resistance in MCF-7 breast cancer cells is associated with altered subcellular localization of p21CIP1 and p27KIP1. Cell Death Differ. 2005;12:98-100.